



Published in final edited form as:

AJNR Am J Neuroradiol. 2017 April ; 38(4): 814–819. doi:10.3174/ajnr.A5097.

White matter tract pathology in pediatric anoxic brain injury from drowning

Mariam Ishaque, PhD^{1,2}, Janessa H. Manning, PhD³, Mary D. Woolsey, MS¹, Crystal G. Franklin, BS¹, Felipe S. Salinas, PhD¹, and Peter T. Fox MD^{1,2,4,5}

¹Research Imaging Institute, University of Texas Health Science Center at San Antonio, San Antonio, Texas, USA

²Department of Radiological Sciences, University of Texas Health Science Center at San Antonio, San Antonio, Texas, USA

³Merrill Palmer Skillman Institute, Wayne State University, Detroit, Michigan, USA

⁴South Texas Veterans Healthcare System, San Antonio, Texas, USA

⁵Shenzhen University School of Medicine, Shenzhen, People's Republic of China

Abstract

Background and Purpose—Although drowning is a leading cause of mortality and morbidity in young children, the neuropathological consequences remain to be fully determined. The purpose of this paper is to quantitatively characterize white matter microstructural abnormalities in pediatric anoxic brain injury (ABI) from nonfatal drowning and investigate correlation with motor function.

Materials and Methods—Whole-brain T1-weighted and diffusion-weighted MRI datasets were acquired in 11 children with chronic ABI and 11 age- and gender-matched neurotypical controls (4-12 years). A systematic evaluation form and scoring system were created to assess motor function. Tract-Based Spatial Statistics (TBSS) was used to quantify between-group alterations in the diffusion tensor imaging indices of fractional anisotropy (FA) and mean diffusivity (MD), and to correlate with per-subject functional motor scores.

Results—Group-wise TBSS analyses demonstrated reduced FA in bilateral posterior limbs of the internal capsule (PLICs) and the splenium of the corpus callosum ($p < 0.001$). MD was more diffusely increased, affecting bilateral superior corona radiata, anterior and posterior limbs of the internal capsule, and external capsules ($p < 0.001$). Individual subject FA and MD values derived from ROIs of bilateral PLICs strongly correlated with motor scores and demonstrated more potent between-group effects than with ROIs of the entire corticospinal tract.

Conclusion—These data particularly implicate the deep white matter, predominantly the PLICs, as targets of damage in pediatric ABI with drowning. The significant involvement of motor-system tracts with relative sparing elsewhere is notable. These results localize white matter pathology and inform future diagnostic and prognostic markers.

Introduction

Drowning is a leading global cause of unintentional injury death and the most important cause in children less than four years of age.¹ Drowning followed by successful cardiopulmonary resuscitation (nonfatal drowning) is also most important in young children, with an estimated 2/3 surviving.^{2,3} In these patients, anoxic brain injury (ABI) ensues from the brain's particular dependence on a continuous oxygen supply, thereby leading to varying levels of neurologic morbidity, and typically, significant motor dysfunction.¹

Although the full extent of neuropathological consequences from ABI in drowning remains to be established, the resultant injury has been characterized as predominantly affecting grey matter (over white matter), largely based on the tissues' metabolic demand profiles.^{4,5} In our recent voxel-based morphometric (VBM) analyses of T1-weighted MR data in children with drowning-related ABI, however, we observed central subcortical tissue loss (in the lenticulostriate arterial distribution) affecting both grey and white matter.⁶ We now aim to specifically assess white matter microstructural integrity in this population using an imaging modality and analysis method more robust for this purpose.

DTI allows *in vivo* assessment of white matter microstructure by measuring water diffusion properties. Tract-based spatial statistics (TBSS) is an optimized DTI method that mediates group-wise, voxel-wise, quantitative white matter analysis.⁷ Here, we use TBSS to measure whole-brain white matter abnormalities and assess motor function correlates in pediatric patients that sustained ABI from drowning. To our knowledge, this is the first study to quantitatively characterize white matter microstructural damage in drowning.

Methods

Participants

Data were acquired from 22 subjects: 11 children with chronic ABI from nonfatal drowning and 11 age- and gender-matched neurotypical controls. Inclusion criteria for ABI patients were (a) a medically stable state, (b) at least six months post injury, (c) no contraindications to MRI, and (d) normal sleep-wake cycles (as children were imaged during sleep). Participant information is shown in Table 1.

All participants' parent(s) provided written consent to the study's protocol, approved by the University of Texas Health Science Center at San Antonio's Institutional Review Board. All participants received a stipend.

Image Acquisition

MRI data were obtained on a 3T Siemens TIM-Trio (Siemens Medical Solutions, Erlangen, Germany), using a standard 12-channel head coil as a radiofrequency receiver and the integrated circularly polarized body coil as the radiofrequency transmitter. T1-weighted images were acquired during mildly sedated sleep (1-2 mg/kg Diphenhydramine HCl) using the MPRAGE pulse sequence with TR / TE = 2200 / 2.72 ms, flip angle = 13°, TI = 766 ms, volumes = 208, and 0.8 mm isotropic voxel size. A single-shot, single refocusing spin-echo, EPI sequence was used to acquire diffusion weighted data with a spatial resolution of 1.7 ×

1.7 × 3 mm. The sequence parameters were: TR / TE = 7800 / 88 ms, FOV = 220 mm, 55 isotropically distributed diffusion weighted directions, two diffusion weighting values, $b = 0$ and 700 s/mm² and three $b = 0$ (non-diffusion-weighted) images.

DTI Preprocessing and Tract-Based Spatial Statistics

Diffusion weighted data were preprocessed using FMRIB's Diffusion Toolbox, part of FMRIB's Software Library (FSL).⁸ Raw diffusion MRI data were corrected for eddy currents and head motion using the Eddy Current Correction tool. Voxel-wise statistical analyses of fractional anisotropy (FA) and mean diffusivity (MD) data were successively carried out using Tract-Based Spatial Statistics (TBSS)⁹ within FSL. FA/MD images were created by fitting a tensor model to the raw diffusion data with DTIFIT, and then brain-extracted using BET.¹⁰ All subjects' FA/MD data were aligned into a common space (Montreal Neurological Institute, MNI) by first using linear registration in FLIRT,^{11,12} external to the TBSS environment, and then by using the nonlinear registration tool FNIRT.^{13,14} FNIRT uses a b-spline representation of the registration warp field.¹⁵ The mean FA/MD images were created and thinned to create mean FA/MD skeletons, which represent the centers of all tracts common to the group. Each subject's aligned FA/MD data were projected onto this skeleton and the resulting data fed into voxel-wise cross-subject statistics. MELODIC's mixture modeling tool¹⁶ was applied to raw *tstat* images to produce false discovery rate (FDR) corrected, thresholded statistical images (Figure 1). For visual purposes, skeletonized results were thickened using FSL's *tbss_fill* tool. Maxima locations were derived from the JHU ICBM-DTI-81 atlas.¹⁷

The final sample consisted of 8 neurotypical and 5 ABI children after exclusion of datasets with excessive motion and/or inadequate registration to the standard template. See Table 1 for participant data.

Functional Assessment

A systematic assessment form with a Likert-type (1-5) scoring system probing motor, sensory, and cognitive aspects of behavior was created, with (1) denoting lowest function and (5) denoting normal function. Data on functional abilities of the children with ABI were collected through initial assessments by a neurologist (P.T.F.) at the time of imaging and subsequently through extensive interviews with the children's family members, nurses, teachers, therapists, etc. In the present study, motor function data was used to assess correlation of behavioral measures with per-subject diffusion imaging parameters (FA and MD) in motor tracts. The motor-system assessment, as follows, was largely derived from extant cerebral palsy gross motor function classification systems¹⁸: (1) No self-mobility, wheelchair transported; (2) Self-mobility in managed situation, wheelchair transported; (3) Effective self-mobility otherwise, not walking (wheelchair, rolling, scooting, etc.); (4) Walking with limitations, including hand-held mobility devices (cane or walker); (5) Walking without limitations. See eTable 1 for individual subject measures.

Correlation Analysis

Two sets of ROI analyses were conducted to study motor tract integrity. The first focused on right and left posterior limbs of the internal capsule (PLICs), with regions derived from our

TBSS analysis of FA data (see Fig. 2A). The second focused on right and left corticospinal tracts (CSTs) within the brain, with regions derived from the JHU White Matter Tractography Atlas¹⁷ and restricted to the white matter skeleton (see Fig. 2B). As the corticospinal tracts carry motor information from the cortex to the spinal cord, they traverse and form a large part of the PLICs. Thus, both sets of ROIs query motor pathway integrity. Individual subjects' mean FA and MD values were extracted from the respective right and left portions of each ROI using FSL's *fsStats* tool. Correlations of these values with motor functional scores were measured as Spearman's rank correlation coefficients in the R statistical software environment. Individual subject motor function scores and DTI indices for the PLICs and CSTs are depicted in Figure 2; correlation coefficients are reported in Table 2.

Results

Voxel-wise TBSS Analyses

Significant regions with decreased FA in the ABI group relative to the neurotypical control group were localized to bilateral PLICs and the splenium of the corpus callosum (right hemisphere) ($p < 0.001$; see Fig. 1A and Table 3). Significant regions with increased MD in the ABI group relative to the neurotypical control group were localized to bilateral superior corona radiata, posterior and anterior limbs of the internal capsules, and external capsules ($p < 0.001$; see Fig. 1B and Table 3). When the statistical threshold was relaxed ($p < 0.01$), the output FA and MD differences remained predominately localized to the aforementioned anatomical regions (see eFigure 1). There were no significant regions of increased FA or decreased MD in the ABI group relative to the neurotypical control group.

ROI Analyses and Correlations

With both sets of PLIC and CST ROIs, high correlations were observed with individual subject FA and MD values and motor function (see Table 3). Higher FA and lower MD in bilateral PLICs and CSTs significantly correlated with higher motor function scores. The strongest correlation with motor function ($\rho = 0.845$) was measured using FA values in the right CST. The weakest correlations with motor function were measured using MD values in right ($\rho = -0.776$) and left ($\rho = -0.777$) CSTs. The test most effective in dissociating patient and control groups was FA analysis of the right and left PLICs, with discrete clusters corresponding to each respective group (see Fig. 2C).

Discussion

White matter microstructural abnormalities in children with ABI from drowning were found to largely implicate deep, central white matter regions. Focal differences in fractional anisotropy were detected in bilateral PLICs and the splenium of the corpus callosum. Focal differences in mean diffusivity were detected in bilateral superior corona radiata, internal capsules, and external capsules. Regions of the white matter skeleton demonstrating significant abnormalities in both diffusion metrics were thus within the internal capsules, and specifically in the posterior limbs. In individual subjects, FA and MD values from both

the PLICs and CSTs highly correlated with corresponding motor function scores, but the PLICs were generally more robust as regions-of-interest.

DTI is a powerful, highly clinically relevant, and readily available method for detecting microscopic changes in tissue architecture. Disruption or loss of white matter structural integrity most often manifests as decreased directionality of diffusion, or decreased fractional anisotropy, and increased water mobility, or increased mean diffusivity. Although a single DTI index (i.e., FA) can be a sensitive biomarker for neuropathology, the use of multiple diffusion indices and knowledge of the underlying disease mechanism mitigate its relatively low specificity.^{19,20}

In pediatric drowning, there is limited knowledge on the extent of brain injury from anoxia, especially in white matter. ABI or hypoxic-ischemic-brain injury (HI-BI) are most often thought to selectively target grey matter due to its increased metabolic demands and higher concentrations of excitatory neurotransmitter receptors.^{4,21} White matter involvement has been much more variable in the majority of anoxic etiologies.²¹ Despite the important role of structural neuroimaging in the clinical management of children with ABI, its utility in exposing consistent damage across patients and identifying potential prognostic markers has been stunted by heavy reliance on visual inspection (of usually subtle/non-specific pathology) and a lack of quantitative, group-wise analyses. Diffusion MRI is the most sensitive of the structural imaging modalities for detection of ABI. It could especially benefit from more rigorous analysis to better localize injury and ascertain prognostic and therapeutic correlates.²¹

Our previous voxel-based morphometric analyses in this cohort demonstrated grey and white matter loss in children with ABI that was highly convergent on central subcortical regions, chiefly comprising the basal ganglia nuclei and the PLICs, and extending to the thalamus, superior corona radiata, and external capsules.⁶ This topography implicates the distribution of the perforating lenticulostriate arteries, an end-arterial system, and thus suggests an important vascular component to the pathophysiology of pediatric drowning.

The present analysis of TBSS in diffusion-MR data entirely supports our white matter VBM findings. In children with ABI, the most affected regions – with reduced FA, increased MD, and the highest average *t* statistic values – were within bilateral PLICs. This data-driven analysis independently confirms pathology of the PLICs using the imaging modality/pulse sequence (DTI) and analytic tool (TBSS) most suited and standardized for the study of white matter structure.⁹ Infarct of the lenticulostriate arteries, from cardiovascular dysfunction and systemic hypotension, thus needs to be seriously considered as a factor in the pathophysiology of pediatric drowning due to the corresponding distribution of tissue damage. Alternatively, however, the white matter tissue loss and microstructural disturbances we have observed could be secondary degeneration to predominant injury in the basal ganglia (i.e., grey matter) from the hypoxic-ischemic insult. Primary versus secondary axonal damage could be differentiated with acute and longitudinal imaging. Primary white matter injury would be appreciated with DWI acutely. Secondary white matter injury would be appreciable after a delay period, likely in the subacute phase,

following the process of grey matter damage. This distinction is not possible in the present cohort with chronic HI-BI.

Regardless of the causality of the observed tissue pathology distribution, the involvement of motor-system components is distinctly striking. The basal ganglia nuclei are integral in motor information transmission and voluntary movement, and the PLICs are largely comprised of corticospinal tract fibers carrying motor information from the primary motor cortex to the spinal cord.^{6,22} Importantly, the prevalent insult to cerebral motor networks reported here is concordant with motor impairments characteristically observed both in this patient population and in our patient cohort. The ages of children at highest risk for drowning (1-4 years; 2.4 year-average in our cohort) may explain these observations to some extent. The maturation of areas serving motor (and sensory) functions is thought to precede that of brain regions underlying higher cognitive functions.²³ Thus, younger children (i.e., as in this population) may sustain less direct injury to higher-order cerebral networks, which remain relatively immature, and greater damage to the more “primitive” and developed motor networks. Nonetheless, the relative sparing of other cerebral networks raises the possibility that these children retain substantial cognitive, perceptual, and emotional capabilities, and that they are unable to effectively convey this functional integrity due to motor-system damage. Further examination of this hypothesis with functional neuroimaging methods is strongly indicated.

In addition to localizing the most consistent pathology in drowning-related pediatric ABI and characterizing the functional correlates group-wise, we report extremely high correlations of imaging metrics with motor function at the individual-subject level. Furthermore, using FA and MD values from right and left PLIC regions-of-interest (derived from FA TBSS analysis) and subjects' motor function scores, complete dissociation of subjects in patient and control groups was possible. This was most effectively conducted in FA data (see Fig. 2). Evaluation of FA and/or MD values using PLIC ROIs may help prognosticate and monitor therapeutic effects in children recovering from drowning. This is especially powerful as each subject could serve as his or her own baseline reference, and longitudinal changes in white matter microstructure could be evaluated for response over time and to interventions. In a perinatal anoxia study, TBSS and diffusion metrics in internal capsule ROIs were indeed able to detect the therapeutic efficacy of hypothermia in infants with neonatal encephalopathy.²⁴ In another study of chronic stroke patients, FA measurements in corticospinal tracts correlated with the potential for motor functional recovery.²⁵ Such analyses would also be feasible and potentially quite useful in the patient population herein described.

To assess the specificity of injury in this cohort, ROI analyses were also implemented in the corticospinal tracts. CST ROIs were derived from a white matter atlas and subjected to the same analysis as the PLIC ROIs. Although high correlations with motor function scores were also measured using the CSTs, they were not as effective in delineating patient and control subjects.

This is not terribly surprising considering the origin of the ROIs: the PLIC regions used in the correlation analysis represent the most significant between-group differences in FA (and

MD), while the CST regions encompass proximal and distal areas as well. The presence (or relative greater quantity) of crossing fibers in the CST ROIs may also in part contribute to this disparity. Injury in pediatric ABI from drowning nevertheless does appear to be most specific to the PLICs.

Several future directions are of importance. Probabilistic diffusion tractography studies are indicated, and quite well informed, by the findings reported here. Probabilistic tractography can be implemented at the per-subject level to obtain connectivity indices reflecting intact fiber organization.²⁶ Although the typical method entails seed-to-target connectivity measurements across a tract (i.e., the entire CST), our results suggest it would be more powerful to measure connectivity across the PLICs. Our findings also prompt future clinical applications in targeted MRS and endovascular therapies to the lenticulostriate arteries via the middle and/or anterior cerebral arteries, as described in Ishaque *et al.*⁶ Further testing is warranted via treatment trails in an anoxic brain injury model in non-human primates.

This study is not lacking in limitations. Diffusion-weighted MRI is known to be extremely sensitive to subject motion, eddy currents, and magnetic field inhomogeneities.¹⁹ Additionally, we were rather stringent with data inclusion to ensure quantitative analysis of high-quality data. This accordingly resulted in the exclusion of 3 control and 6 ABI datasets, either due to excessive motion in the first instance or inadequate registration within the TBSS analysis thereafter. Thus, we acknowledge that our findings are from a small sample size. Diffusion MR data acquisition would likely benefit from increased sedation of pediatric subjects. We emphasize, however, that substantial (and focal) between-group differences were nevertheless observed at quite high statistical significance levels. We are thereby confident that our findings reflect underlying disease-specific white matter pathology. With that being said, we do interpret our results as specific to pediatric ABI from drowning and recognize they may not generalize to other anoxic etiologies or age groups. For clinical purposes, the group-wise study design we use is also a limitation. An alternative for future exploration would be per-subject probabilistic tractography, as discussed above. The most promising method as we see it would involve tractography of the PLICs.

Conclusion

This study reports the first quantitative, whole-brain, voxel-wise characterization of white matter microstructural changes in pediatric ABI from drowning. TBSS analysis of FA and MD indices demonstrated substantial disruption of the deep, central white matter, predominantly implicating motor tracts; these results significantly correlated with motor functional abilities at the individual-subject level. Other white matter tracts were observed to be relatively preserved. These findings support our recent grey and white matter VBM analyses that localized structural pathology to the basal ganglia and internal capsules, and together, suggest primary motor-system damage in this population. The prospect of motor nuclei/motor pathway injury masking relatively intact cognitive, perceptual, and emotional abilities in children with ABI from drowning must be further investigated. Additionally, our reported results motivate important diagnostic, prognostic, and therapeutic considerations.

Supplementary Material

Refer to Web version on PubMed Central for supplementary material.

Acknowledgments

The authors thank all families for their time and participation in this study. The authors thank Dr. Christian F. Beckmann, Ph.D. (University of Oxford; Donders Institute) for his data analysis suggestions.

This work was supported by the NIH (R01 MH074457; TL1 TR001119) and the Kronkosky Charitable Foundation. The Conrad Smiles Fund (www.conradsmiles.org) publicized this study and provided funding for travel and logistical support. Miracle Flights for Kids supported airfare costs where possible.

References

1. Topjian AA, Berg RA, Bierens JJLM, et al. Brain Resuscitation in the Drowning Victim. *Neurocrit Care*. 2012; 17:441–67. [PubMed: 22956050]
2. Borse N, Sleet DA. CDC Childhood Injury Report: Patterns of Unintentional Injuries Among 0- to 19-Year Olds in the United States, 2000-2006. *Fam Community Health*. 2009; 32:189–9. [PubMed: 19305217]
3. Kriel RL, Krach LE, Luxenberg MG, et al. Outcome of severe anoxic/ischemic brain injury in children. *Pediatric Neurology*. 1994; 10:207–12. [PubMed: 8060422]
4. Huang BY, Castillo M. Hypoxic-ischemic brain injury: imaging findings from birth to adulthood. *RadioGraphics*. 2008; 28:417–617. [PubMed: 18349449]
5. Hegde AN, Mohan S, Lath N, et al. Differential diagnosis for bilateral abnormalities of the basal ganglia and thalamus. *RadioGraphics*. 2011; 31:5–30. [PubMed: 21257930]
6. Ishaque M, Manning JH, Woolsey MD, et al. Lenticulostriate arterial distribution pathology may underlie pediatric anoxic brain injury in drowning. *NeuroImage: Clinical*. 2016; 11:167–72. [PubMed: 26937385]
7. Smith SM, Jenkinson M, Johansen-Berg H, et al. Tract-based spatial statistics: Voxelwise analysis of multi-subject diffusion data. *Neuroimage*. 2006; 31:1487–505. [PubMed: 16624579]
8. Smith SM, Jenkinson M, Woolrich MW, et al. Advances in functional and structural MR image analysis and implementation as FSL. *Neuroimage*. 2004; 23(1):S208–19. [PubMed: 15501092]
9. Smith SM, Jenkinson M, Johansen-Berg H, et al. Tract-based spatial statistics: Voxelwise analysis of multi-subject diffusion data. *Neuroimage*. 2006; 31:1487–505. [PubMed: 16624579]
10. Smith SM. Fast robust automated brain extraction. *Hum Brain Mapp*. 2002; 17:143–55. [PubMed: 12391568]
11. Jenkinson M, Smith S. A global optimisation method for robust affine registration of brain images. *Medical Image Analysis*. 2001; 5:143–56. [PubMed: 11516708]
12. Jenkinson M, Bannister P, Brady M, et al. Improved Optimization for the Robust and Accurate Linear Registration and Motion Correction of Brain Images. *Neuroimage*. 2002; 17:825–41. [PubMed: 12377157]
13. Andersson, J., Jenkinson, M. University of Oxford FMRIB 2007. Non-linear optimisation FMRIB technical report TR07JA1. Epub ahead of print
14. Andersson J, Jenkinson M, Smith S. Non-linear registration, aka Spatial normalisation FMRIB technical report TR07JA2. FMRIB Analysis Group of 2007 Epub ahead of print.
15. Rueckert D, Sonoda LI, Hayes C, et al. Nonrigid registration using free-form deformations: application to breast MR images. *Medical Imaging, IEEE Transactions on*. 1999; 18:712–21.
16. Woolrich MW, Behrens TEJ, Beckmann CF, et al. Mixture models with adaptive spatial regularization for segmentation with an application to FMRI data. *Medical Imaging, IEEE Transactions on*. 2005; 24:1–11.
17. Mori, S. MRI Atlas of Human White Matter. Elsevier Science Limited; 2005.

18. Palisano R, Rosenbaum P, Walter S, et al. Development and reliability of a system to classify gross motor function in children with cerebral palsy. *Developmental Medicine & Child Neurology*. 1997; 39:214–23. [PubMed: 9183258]
19. Alexander AL, Lee JE, Lazar M, et al. Diffusion tensor imaging of the brain. *Neurotherapeutics*. 2007; 4:316–29. [PubMed: 17599699]
20. Yamada K, Sakai K, Akazawa K, et al. MR tractography: a review of its clinical applications. *Magn Reson Med Sci*. 2009; 8:165–74. [PubMed: 20035125]
21. Rabinstein, AA., Resnick, SJ. *Practical Neuroimaging in Stroke*. Elsevier Health Sciences; 2009.
22. Anderson JC, Costantino MM, Stratford T. Basal ganglia: anatomy, pathology, and imaging characteristics. *Current Problems in Diagnostic Radiology*. 2004; 33:28–41. [PubMed: 14712200]
23. de Bie HMA, Boersma M, Adriaanse S, et al. Resting-state networks in awake five- to eight-year old children. *Hum Brain Mapp*. 2012; 33:1189–201. [PubMed: 21520347]
24. Porter EJ, Counsell SJ, Edwards AD, et al. Tract-based spatial statistics of magnetic resonance images to assess disease and treatment effects in perinatal asphyxial encephalopathy. *Pediatr Res*. 2010; 68:205–9. [PubMed: 20520585]
25. Stinear CM, Barber PA, Smale PR, et al. Functional potential in chronic stroke patients depends on corticospinal tract integrity. *Brain*. 2007; 130:170–80. [PubMed: 17148468]
26. Behrens TEJ, Berg HJ, Jbabdi S, et al. Probabilistic diffusion tractography with multiple fibre orientations: What can we gain? *Neuroimage*. 2007; 34:144–55. [PubMed: 17070705]

Abbreviations

ABI	anoxic brain injury
CST	corticospinal tract
FA	fractional anisotropy
FDR	false discovery rate
HI-BI	hypoxic-ischemic-brain injury
MD	mean diffusivity
MNI	Montreal Neurological Institute
PLIC	posterior limb of the internal capsule
TBSS	tract-based spatial statistics
VBM	voxel-based morphometry

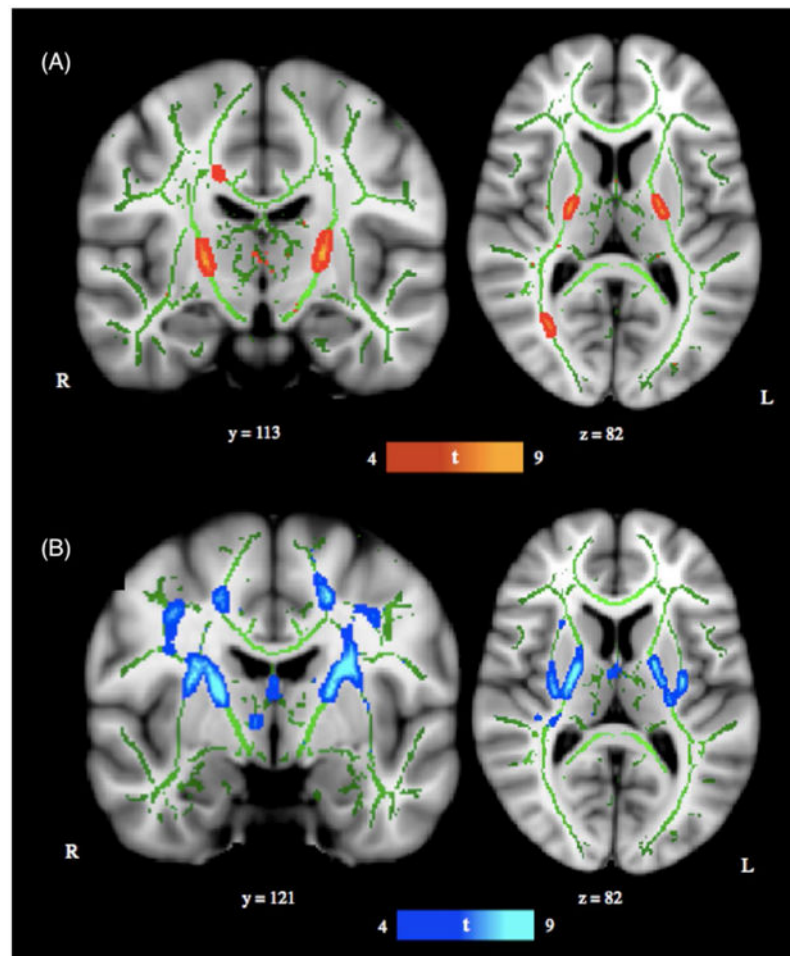


Figure 1. TBSS Results

(A) TBSS derived t -map of decreased fractional anisotropy (FA) in the anoxic brain injury (ABI) group relative to the neurotypical control group is shown in red-yellow ($p < 0.001$; corrected for multiple comparisons). (B) TBSS derived t -map of increased mean diffusivity (MD) in the ABI group relative to the neurotypical control group is shown in blue-light blue ($p < 0.001$; corrected for multiple comparisons). Results were thickened with *tbss_fill* and are overlaid onto study-specific white matter skeleton (green) and the Montreal Neurological Institute's (MN1-152) template. Slice position (given by y or z location) corresponds to MN1-152 template space.

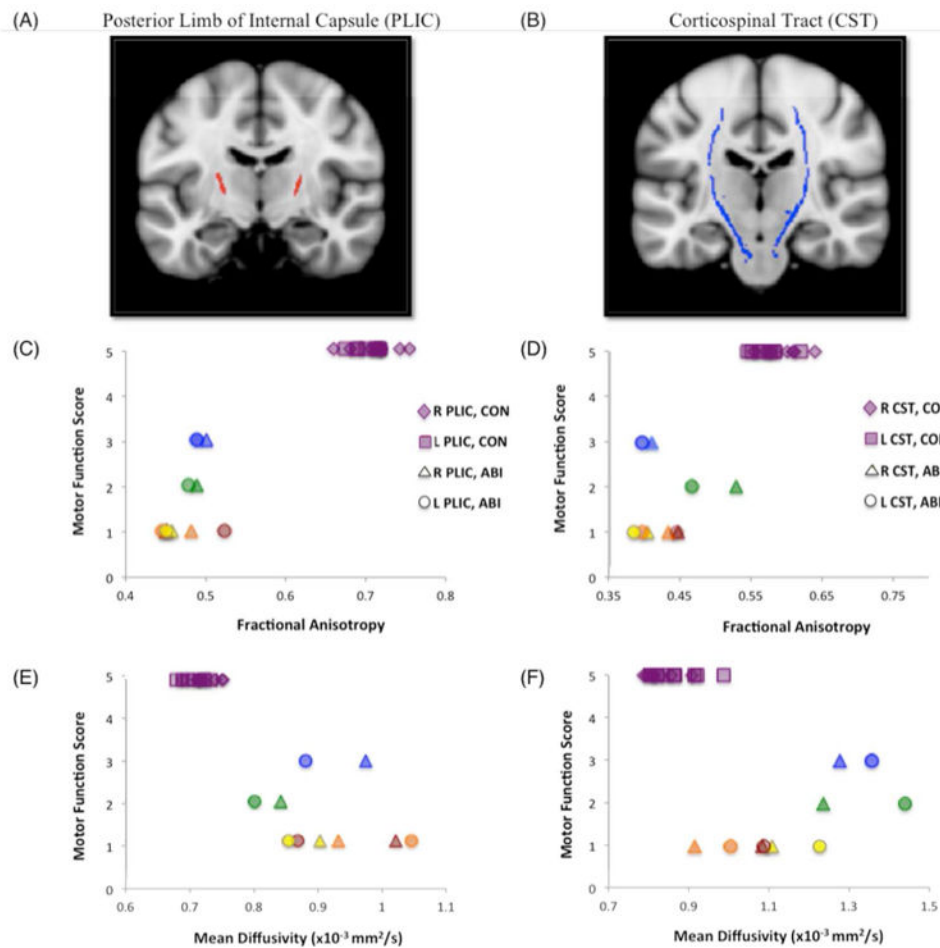


Figure 2. Motor Function Scores versus Diffusion Indices

Scatterplots of per-subject motor function scores versus per-subject mean fractional anisotropy (FA) and mean diffusivity (MD) values from region-of-interest (ROI) analyses of (A) the right and left posterior limbs of the internal capsule (PLICs, red), and (B) the right and left corticospinal tracts (CSTs, blue), are shown. Motor scores are derived from our functional assessment forms; PLIC ROIs were derived from clusters in our TBSS analysis of FA data; CST ROIs were derived from the JHU White Matter Tractography Atlas. ABI patient data is color-coded per subject for bilateral PLICs and CSTs: blue = patient A; green = patient B; yellow = patient C; orange = patient D; red = patient E. (C) Motor function scores versus FA, right and left PLICs; (D) Motor function scores versus FA, right and left CSTs; (E) Motor function scores versus MD, right and left PLICs; (F) Motor function scores versus MD, right and left CSTs. Analysis of FA data in bilateral PLICs demonstrates the strongest between-group effects (at the individual subject level), fully differentiating control (CON) and anoxic brain injury (ABI) subjects.

Table 1**Participant Information**

Information from all participants and those included in the present study.

Group	Sex (M/F)	Age at Injury (years) (mean \pm SD^I)	Age at Scan (years) (mean \pm SD^I)	Time Since Injury (years) (mean \pm SD^I)
All ABI n=11	8/3	2.5 \pm 1.1	7.7 \pm 2.9	5.2 \pm 3.1
All Control n=11	8/3	-	7.2 \pm 2.2	-
Incl. ABI n=5	3/2	2.4 \pm 0.8	6.7 \pm 2.8	4.3 \pm 2.2
Incl. Control n=8	6/2	-	6.9 \pm 2.4	-

^I standard deviation

Author Manuscript

Author Manuscript

Author Manuscript

Author Manuscript

Table 2
Motor Function Correlation with Diffusion Indices

Spearman's rank correlation coefficients (ρ) between per-subject motor scores and fractional anisotropy or mean diffusivity values from ROI-analyses of right and left posterior limbs of the internal capsule (PLICs, $p < 0.001$) and corticospinal tracts (CSTs, $p < 0.005$) are reported.

Region of interest	Spearman's ρ	
	Fractional anisotropy	Mean diffusivity
Right PLIC	0.807 ($p < 0.001$)	- 0.827 ($p < 0.001$)
Left PLIC	0.814 ($p < 0.001$)	- 0.827 ($p < 0.001$)
Right CST	0.845 ($p < 0.005$)	- 0.776 ($p < 0.005$)
Left CST	0.807 ($p < 0.005$)	- 0.777 ($p < 0.005$)

Table 3**TBSS Results**

Location and coordinates of peaks of significant white matter abnormalities in fractional anisotropy and mean diffusivity are reported ($p < 0.001$, clusters $> 100 \text{ mm}^3$). White matter tissue labels derived from JHU ICBM-DTI-81 atlas.

Anatomical location	Hemisphere	MNI coordinates of global maxima		
		x	y	z
Fractional Anisotropy				
<i>Control > ABI</i>				
Posterior Limb of Internal Capsule	L	-22	-12	7
Posterior Limb of Internal Capsule	R	20	-8	8
Corpus Callosum, Splenium	R	20	-38	31
Mean Diffusivity				
<i>ABI > Control</i>				
Superior Corona Radiata	R	27	-8	44
Superior Corona Radiata	L	-21	-24	43
Internal Capsule	R	25	2	20
Internal Capsule	L	-26	-2	22
External Capsule	R	29	-6	18
External Capsule	L	-32	-11	9